

# Nanostructures Generated from Photopolymerization of Poly(ethylene glycol) Diacrylate Templated from Hexagonal Lyotropic Liquid Crystals

Juan Zhang,<sup>1,2</sup> Zongli Xie,<sup>2</sup> Feng Hua She,<sup>1</sup> Manh Hoang,<sup>2</sup> Anita J. Hill,<sup>2</sup> Wei Min Gao,<sup>1</sup> Ling Xue Kong<sup>1</sup>

<sup>1</sup>Centre for Material and Fibre Innovation, Deakin University, Geelong, Victoria, Australia

<sup>2</sup>CSIRO Material Science and Engineering, Clayton, Victoria, Australia

Received 16 June 2010; accepted 12 September 2010

DOI 10.1002/app.33397

Published online 1 December 2010 in Wiley Online Library (wileyonlinelibrary.com).

**ABSTRACT:** The use of lyotropic liquid crystals (LLC) as a template to form periodic nanostructures in polymer materials is a promising technology. In this study, cross-linked poly(ethylene glycol) diacrylate nanostructured materials were prepared by photopolymerization in LLC hexagonal phases. Polarized light microscopy and small-angle powder X-ray diffraction were used to understand the original LLC order retention on photopolymerization, and scanning electron microscope was used to investigate the morphology under different purifying solvents and drying conditions. A Quantachrome Autosorb 1 system was used

to study the pore size distribution of samples. It was found that the LLC hexagonal structure was retained to a great extent after photopolymerization. The formation of nanostructures was affected by purifying solvent and drying condition. The nanostructure synthesized from LLC with favorably aligned nanopores will find increasing applications in gas and water filtration, biology, and health science. © 2010 Wiley Periodicals, Inc. *J Appl Polym Sci* 120: 1817–1821, 2011

**Key words:** nanotechnology; lyotropic liquid crystals; phase behavior; photopolymerization

## INTRODUCTION

Controlling the size and distribution of interstitial voids or nanopores in nanofiltration (NF) membranes is crucial to the selectivity, filtration efficiency, and energy consumption.<sup>1–3</sup> An NF polymer membrane with aligned nanopores perpendicular to the membrane surface will improve the flow rate and reduce the energy consumption associated with the water treatment and desalination processes.

Carbon nanotubes have perfect atomic dimensions and atomic smoothness, representing a potential unique family of materials for controlled flow. The ideal orientation of nanopores such as single-walled carbon nanotubes<sup>2</sup> and multiwalled carbon nanotubes<sup>4</sup> can significantly improve the gas and water permeabilities of these nanotube-based membranes. However, the extraordinarily high cost involved in fabricating this kind of membranes has encouraged the exploration of other materials with equivalent structural advantage but less expensive to be synthesized.

Lyotropic liquid crystals (LLC) exhibit periodic nanostructures (ranging from micelles, lamellar, hexagonal, to bicontinuous) depending on concentration and temperature. The hexagonal LLC phases have molecular aggregate ordering that corresponds to a hexagonal arrangement.<sup>5</sup> The diameter of the hexagonal cylinders is generally less than 10 nm, which is the typical pore size of NF membranes. Studies on hexagonal LLC template in inorganic<sup>6–8</sup> and organic materials<sup>9–12</sup> to generate ordered nanostructures have attracted a great deal of interest in recent years. However, templating the hexagonal LLC nanostructures onto polymer membranes for water treatment has been rarely reported. Zhou et al.<sup>13</sup> used the polymerizable ionic amphiphiles, which itself acted as both the surfactant and the monomer, to generate the nanostructured NF membrane. Although the reported water flux of this membrane was quite low, the LLC renders a promising technology that can generate pores of nanodimension and controllable orientation for high flux gas and water transport.

In our study, the hexagonal LLC phase was used as the sacrificed template to generate cylindrical pores in polymer materials. Figure 1 represents the main LLC templating process: first dispersing the surfactants in monomers to form hexagonal phase, then photopolymerizing the monomers followed by surfactant removal, and finally achieving nanoporous structure with cylindrical pores. Photopolymerization method was chosen because it offers

Correspondence to: L. X. Kong (lingxue.kong@deakin.edu.au).

Contract grant sponsors: Deakin University Postgraduate Scholarship, Australian CSIRO Water for a Healthy Country Flagship Top-Up Scholarship.

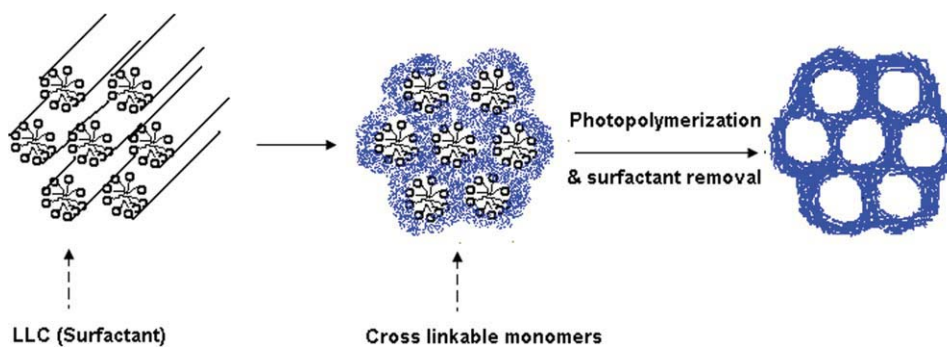


**Figure 1** Representative LLC templating process. [Color figure can be viewed in the online issue, which is available at [wileyonlinelibrary.com](http://wileyonlinelibrary.com).]

extremely rapid initiation rate, which enables better template structure retention by allowing the growing polymer to do significant cross-linking before phase separation can happen.<sup>14</sup>

The retention of original LLC structure on polymerization and after surfactant removal has been

one of the key issues in this research field. The aim of this study was to investigate the retention of LLC structure on polymerization and the effects of purifying solvents and drying conditions on nanostructure generation. A highly cross-linked poly(ethylene glycol) diacrylate (PEGDA) was photopolymerized in hexagonal LLC mesophases formed from Brij56

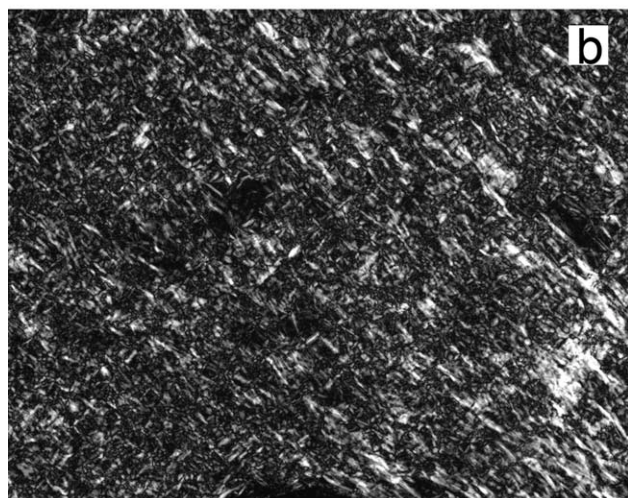
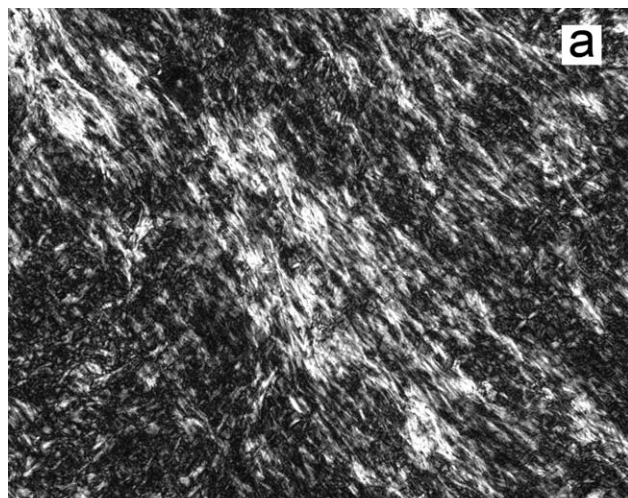


**Figure 2** Polarized light microscopy images of the samples: (a) before and (b) after photopolymerization in hexagonal phases formed from Brij 56/water system.

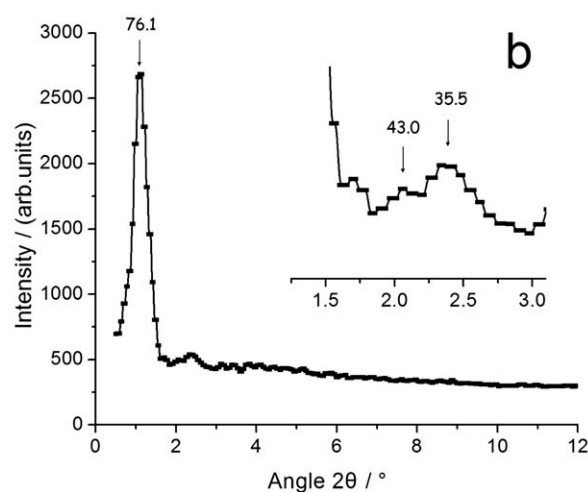
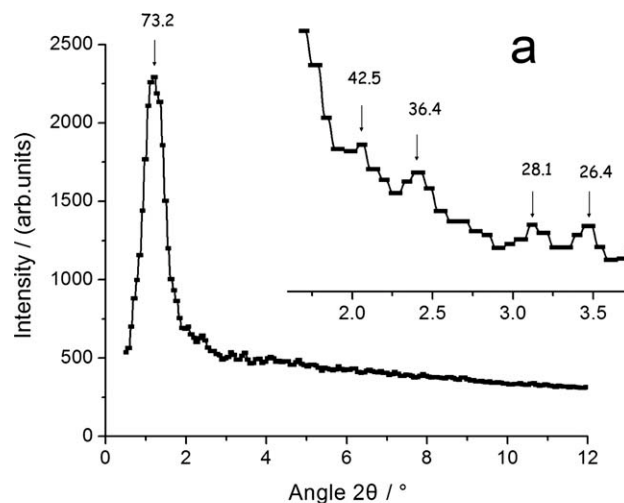


**Figure 3** XRD profiles of samples: (a) before and (b) after polymerization in the hexagonal phases formed from Brij 56/water system.

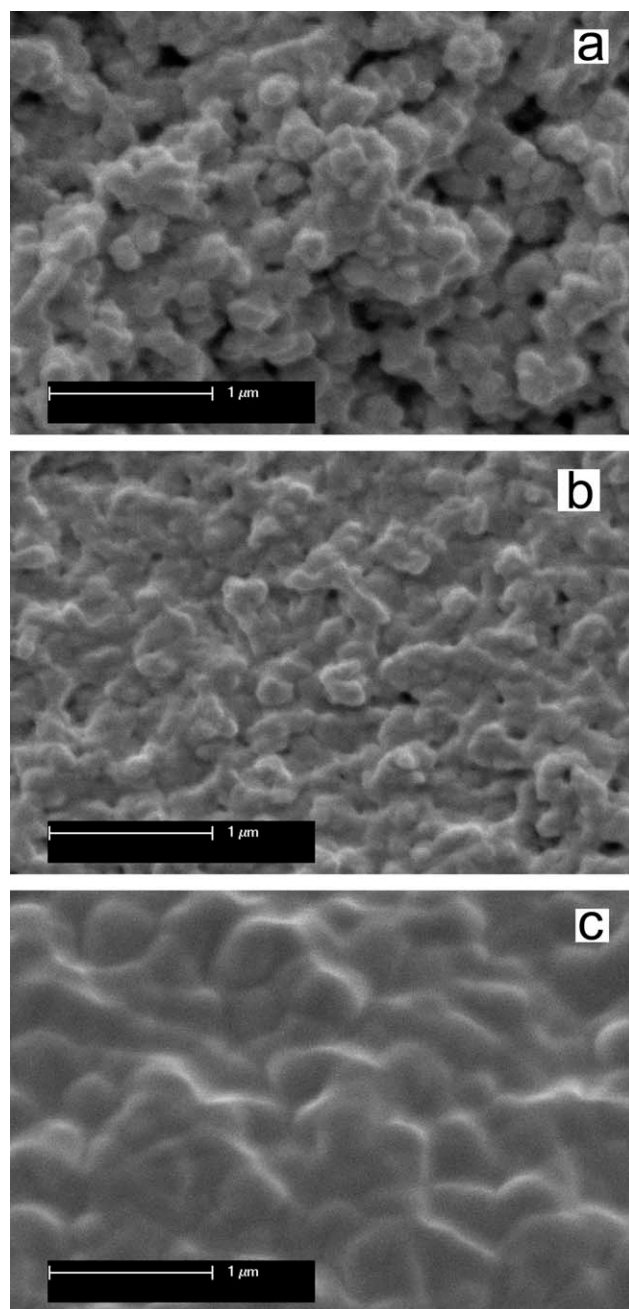


**Figure 4** Cross-sectional scanning electron microscopy images of dried samples: (a) purified by ethanol and dried in air; (b) purified by ethanol and dried in vacuum oven; and (c) purified by distilled water and dried in vacuum oven.

surfactant and water system. The samples were purified using different solvents and dried under different conditions.

## EXPERIMENTAL

### Materials

PEGDA ( $n = 11$ , molecular weight = 575 g/mol), 2-hydroxyl-2-methylpropiophenone (97%), Brij 56, and

2-hydroxy-2-methylpropiophenone (97%) were purchased from Sigma-Aldrich (St. Louis, MO). All chemicals were used as received.

### Synthesis

All LLC solutions were synthesized by mixing PEGDA/Brij56/2-hydroxy-2-methylpropiophenone/deionized water in a ratio of 40/35/0.5/24.5 (by weight). Mixture was stirred in a 50°C water bath for 20 min to obtain a homogenous solution, which was then cast on a glass sheet. The samples were sealed in a glove box under argon atmosphere before being placed under a 300–400 nm ultraviolet light source (intensity 2.0 mW/cm<sup>2</sup>, 10 min) for photopolymerization. After polymerization, the samples were purified by distilled water or absolute ethanol to remove Brij 56 and unreacted monomer, and then dried either in a vacuum oven or in air at room temperature.

### Characterization

Polarized light microscope (Olympus BH2-UMA) was used to characterize textures of the mesophase of samples before and after photopolymerization. Powder X-ray diffraction (XRD) was used to examine the phase behavior of the samples before and after photopolymerization. It was conducted using a Bruker AXS diffractometer with a Cu K $\alpha$  radiation operating at 40 kV, 40 mA under transmission mode. Scanning electron microscopy (ESEM Philips XL30) was used to characterize sample morphology. Differential scanning calorimetry (TA DSC Q200) was used to determine the glass-transition temperatures ( $T_g$ ) of untemplated cross-linked PEGDA and templated samples. The analysis was conducted under nitrogen and at a scan rate of 10°C min<sup>-1</sup>.

The pore size distributions of the samples were characterized with a Quantachrome Autosorb 1 system by using nitrogen as an adsorbent at liquid nitrogen temperature. Barrett–Joyner–Halenda method on desorption data was used to work out the pore size distribution.

The water uptake was determined as follows: the dried samples were weighed first, and then were soaked in deionized water for 2 h. After that, the samples were taken out from water and weighed immediately after blotting the free water on the surface. Water uptake was calculated according to the following equation:

$$\text{Water uptake} = \frac{(W_s - W_d)}{W_d} \times 100\%$$

where  $W_s$  and  $W_d$  are the weights of swollen and dry cross-linked PEGDA samples, respectively.

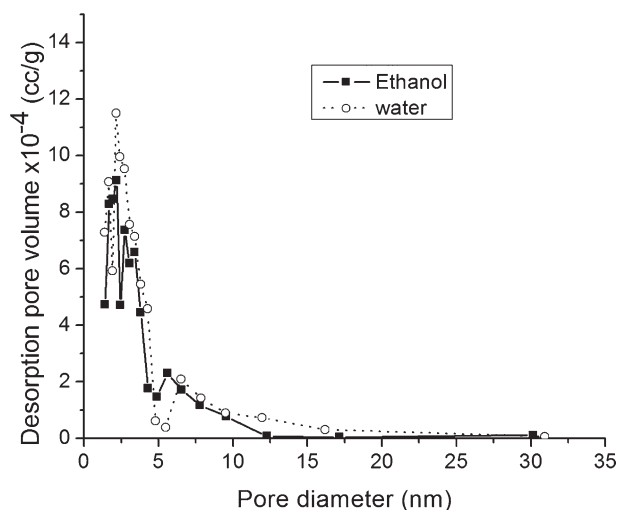


**Figure 5** Barrett-Joyner-Halenda desorption pore size distribution of samples purified by ethanol and water, respectively. Both samples were dried in vacuum oven.

## RESULTS AND DISCUSSION

In this study, a highly cross-linked PEGDA was photopolymerized in hexagonal LLC mesophases formed from Brij 56 surfactant and water system. To gain better understanding of the original LLC order retention on photopolymerization, polarized light microscopy and XRD were used to observe the phase behavior before and after polymerization. Figure 2 shows the polarized light micrographs before [Fig. 2(a)] and after [Fig. 2(b)] polymerization. Before polymerization, a focal conic texture was observed, indicating the presence of a hexagonal mesophase.<sup>12,15</sup> After polymerization, the sample remained in a focal conic texture, though it was slightly coarsened. There was no apparent phase separation on cure, indicating that the original LLC structure is retained to a great extent.

Figure 3 shows the XRD profiles of samples before and after polymerization. The observed  $d$ -spacing ratios of 1,  $1/3^{1/2}$ ,  $1/4^{1/2}$ ,  $1/5^{1/2}$ , and  $1/7^{1/2}$  in the sample before polymerization and 1,  $1/3^{1/2}$ , and  $1/5^{1/2}$  in the sample after polymerization are characteristic of the hexagonal LLC phase.<sup>16,17</sup> This is in good agreement with the polarized light microscopy results, i.e., the original LLC order is retained to a great extent after photopolymerization.

It is believed that purifying solvent and drying conditions affect the morphology of samples. A series of samples were prepared by using different purifying solvents and dried at different conditions. Figure 4(a,b) shows the morphologies of samples purified using absolute ethanol but dried under different conditions. The sample dried in air shows an irregular porous structure, whereas that dried in the vacuum oven has a denser structure. The sample dried in the vacuum oven might result in a less

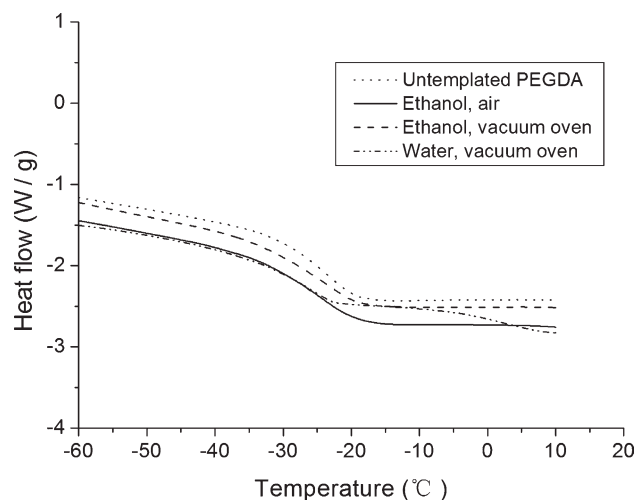


**Figure 6** Differential scanning calorimetry test of untemplated cross-linked PEGDA and templated samples purified by ethanol and dried in air; purified by ethanol and dried in vacuum oven; and purified by water and dried in vacuum oven, respectively.

chance for rearranging the polymer chains. When the sample is dried in air, some small pores might collapse, leading to the formation of large pores.

Figure 4(b,c) shows the morphologies of samples purified by different solvents and dried in vacuum oven. Both samples have a dense morphology. The pore size distribution of these two samples is shown in Figure 5. The sample purified by ethanol has a pore size distribution between 1.4 and 12 nm, whereas the membrane purified using water has a broader pore size distribution between 1.4 and 22 nm. It is possible that the lower solubility of Brij 56 in water may accelerate the polymer arrangement.

Thermal properties of the untemplated and templated cross-linked PEGDA samples were studied by differential scanning calorimetry. Figure 6 shows the differential scanning calorimetry thermal graphs of

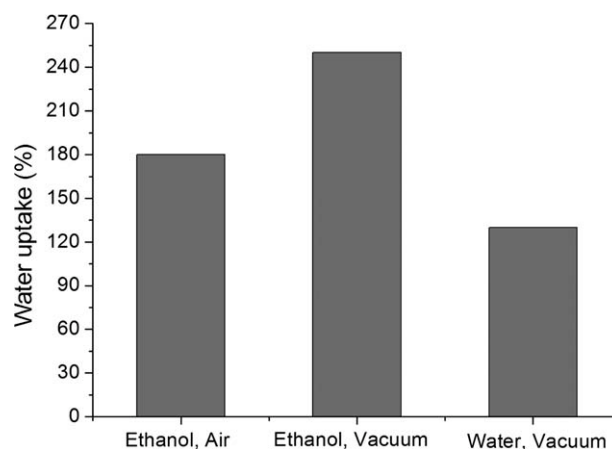


**Figure 7** Water uptakes of samples prepared with different purification and drying conditions.

samples prepared under different conditions. It was found that purifying solvent and drying conditions have no significant influence on glass-transition temperature ( $T_g$ ). Furthermore, the LLC templating also has little influence on  $T_g$ . The  $T_g$  of untemplated cross-linked PEGDA is  $-24^\circ\text{C}$ , the templated sample purified by ethanol and dried in vacuum oven is  $-25^\circ\text{C}$ , and the other two samples  $-26^\circ\text{C}$ . The low  $T_g$  of this material represents high chain mobility, which, in turn, facilitates the polymer rearrangement during the removal of Brij 56 and drying process.

Figure 7 shows the water uptake of samples prepared under different conditions. It can be found that water uptake of the sample purified using ethanol and dried in air is 180 wt %, whereas the one dried in vacuum oven is 250%, which is 70% higher, though the former sample is more porous as shown in scanning electron microscopy images (Fig. 4). The sample purified by water has the lowest water uptake, only 130%. Previous research has shown that a higher water uptake would indicate more ordered hexagonal structure.<sup>12</sup> The sample purified using ethanol and dried in the vacuum oven has the highest water uptake, which implies this sample has a better nanostructure than other samples. This is in agreement with the narrow pore size distribution (Fig. 5).

## CONCLUSIONS

The hexagonal phase was successfully formed in LLC solution and was retained to a great extent after photopolymerization. The sample morphology is affected by the purified solvents and drying conditions. The sample purified with ethanol and dried in vacuum oven has good nanostructure with a narrow

pore size distribution and a high water uptake, implying high water permeability of this kind of material for the potential application of water treatment. Purifying solvents and drying conditions have no significant influence on glass-transition temperature ( $T_g$ ). Furthermore, the LLC templating also has little influence on  $T_g$ .

## References

1. Ulbricht, M. *Polymer* 2006, 47, 2217.
2. Holt, J. K.; Park, H. G.; Wang, Y. M.; Stadermann, M.; Artyukhin, A. B.; Grigoropoulos, C. P.; Noy, A.; Bakajin, O. *Science* 2006, 312, 1034.
3. Yang, S. Y.; Ryu, I.; Kim, H. Y.; Kim, J. K.; Jang, S. K.; Russell, T. P. *Adv Mater* 2006, 18, 709.
4. Majumder, M.; Chopra, N.; Andrews, R.; Hinds, B. J. *Nature* 2005, 438, 44.
5. Collings, P. J.; Hird, M. *Introduction to Liquid Crystals: Chemistry and Physics*; Taylor & Francis: Great Britain, 1997.
6. Goltner, C. G.; Berton, B.; Kramer, E.; Antonietti, M., *Adv Mater* 1999, 11, 395.
7. El-Safty, S. A.; Mizukami, F.; Hanaoka, T. *J Phys Chem B* 2005, 109, 9255.
8. Su, B.; Lu, X. M.; Lu, Q. H. *J Am Chem Soc* 2008, 130, 14356.
9. Jahn, W.; Strey, R. *J Phys Chem* 1988, 92, 2294.
10. Antonietti, M.; Hentze, H. P. *Colloid Polym Sci* 1996, 274, 696.
11. Clapper, J. D.; Guymon, C. A. *Macromolecules* 2007, 40, 1101.
12. Sievens-Figueroa, L.; Guymon, C. A. *Chem Mater* 2009, 21, 1060.
13. Zhou, M. J.; Kidd, T. J.; Noble, R. D.; Gin, D. L. *Adv Mater* 2005, 17, 1850.
14. Clapper, J. D.; Sievens-Figueroa, L.; Guymon, C. A. *Chem Mater* 2008, 20, 768.
15. Clapper, J. D.; Guymon, C. A. *Adv Mater* 2006, 18, 1575.
16. Verlooy, P.; Aerts, A.; Lebedev, O. I.; Van Tendeloo, G.; Kirschhock, C.; Martens, J. A. *Chem Commun* 2009, 4287.
17. Gin, D. L.; Gu, W. Q.; Pindzola, B. A.; Zhou, W. J. *Acc Chem Res* 2001, 34, 973.